2011

An In Vitro Comparison of Cyclic Fatigue of Profile® Vortex™ and Endosequence™ Rotary Nickel-Titanium Files

Fawaz Al-Foraih
Virginia Commonwealth University

An *In Vitro* Comparison of Cyclic Fatigue of Profile® Vortex™ and Endosequence™ Rotary Nickel-Titanium Files

A thesis submitted in partial fulfillment of the requirements for the degree of Master of Science in Dentistry at Virginia Commonwealth University.

by

Fawaz T. Al-Foraih,
DDS, Virginia Commonwealth University, School of Dentistry, 2006

Director: Karan J. Replogle, DDS, MS
Department Chair, Department of Endodontics
Virginia Commonwealth University School of Dentistry

Virginia Commonwealth University
Richmond, Virginia
April 7, 2011

Acknowledgment

The author wishes to thank several people. I would like to thank the Ministry of Health, Kuwait for their financial support, my parents for their unending love and support, and Drs. Replogle, Archer, Moon, Best and Al-Ali for their help and direction with this project. Moreover, I would like to offer my gratitude to the American Association of Endodontists (AAE) Foundation for their generous research grant as well as Tulsa Dentsply Dental Specialties and Brasseler, USA for providing their products for research purposes.

Table of Contents

List of Tables

Table Page

List of Figures

Figure Page

Abstract

AN *IN VITRO* COMPARISON OF CYCLIC FATIGUE OF PROFILE® VORTEX™ AND ENDOSEQUENCE™ ROTARY NICKEL-TITANIUM FILES

By Fawaz T. Al-Foraih, DDS

A thesis submitted in partial fulfillment of the requirements for the degree of Master of Science in Dentistry at Virginia Commonwealth University.

Virginia Commonwealth University, 2011.

Program Director: Karan J. Replogle DDS, MS,
Chair and Postgraduate Program Director, Endodontics

The purpose of this study was to determine the number of rotations to fracture (cyclic fatigue) of the Profile® Vortex™ files (Dentsply Tulsa Dental Specialties**,** Tulsa, OK) compared to the EndoSequence™ files (Brasseler USA, Savannah, GA) using an *in-vitro* apparatus simulating a curved canal. Two hundred Profile® Vortex™ files of 25mm length were divided equally into ten groups, one for each of the Profile® Vortex™ files 20/0.04, 20/0.06, 25/0.04, 25/0.06, 30/0.04, 30/0.06, 35/0.04, 35/0.06, 40/0.04, and 40/0.06. Two hundred EndoSequence™ files of 25mm length were divided equally into ten groups of the same tip and taper sizes analogous to the Profile® Vortex™ file groups.

Files were rotated at 500 rpm in a fixed groove in the metal block of the apparatus. The angle of deflection for all files was fixed at 33 degrees, determined using the Schneider method.

The time from initiation of rotation to fracture was recorded and rotations to fracture were calculated.

The data collected was analyzed using a multi-way ANOVA, followed by specific post-hoc contrasts comparing the two brands for each tip and taper combination. The results demonstrated that the Profile® Vortex™ files required significantly greater rotations to fracture than the EndoSequence™ ($p < 0.001$) in all tip sizes in both 0.04 and 0.06 tapers. Profile® Vortex™ files exhibited a greater resistance to cyclic fatigue than the EndoSequence™ files.

Introduction

The objectives of endodontic therapy are to thoroughly clean and shape the root canal system while maintaining its natural anatomy and contours. Upon completion of cleaning and shaping, a three dimensional filling can be applied to the root canal system to seal the prepared canal (1, 2). The cleaning and shaping phase (canal preparation) is accomplished through chemomechanical preparation. This step represents an essential part of root canal therapy (3). Chemomechanical preparation utilizes both the mechanical action of the endodontic instruments and the chemical flushing action of irrigants to disinfect the canal and dissolve organic pulpal remnants (4-6).

Iatrogenic procedural errors during endodontic instrumentation can result in the unsuccessful cleaning of the apical portion of the canal, leading to persistent infection of the root canal system (3, 7). Procedural errors during endodontic instrumentation include apical ledges, zips, perforations and transportation in curved canals (8).

Civjan et al studied the mechanical properties of nickel titanium (NiTi) alloys 55-Nitinol and 60-Nitinol in 1975 and suggested its future use in the fabrication of instruments in the medical and dental field (9). However, the application of Nitinol nickel titanium (NiTi) to endodontic instruments has been credited to Walia et al in 1988. This offered a promising new advancement in canal instrumentation (10). When used ideally, the combination of Nitinol nickel titanium files (NiTi) with rotary instrumentation decreases procedural errors during

instrumentation, especially transportation in curved canals (11). This was attributed to Nitinol's superior elastic flexibility and enhanced resistance to torsion compared to stainless steel files that were previously used to instrument canals (10). Despite the increased flexibility and greater resistance to fracture, separation of the nickel titanium (NiTi) file can and does occur (12, 13). Furthermore, they can fracture within their elastic limit and without visible signs of file deformation (14, 15). If separation of a NiTi file occurs in the confines of the canal, the success rate of endodontic therapy can diminish depending on the preoperative status of the case (16-19).

Rotary NiTi files are subject to two different kinds of stresses (torsional and cyclic) during instrumentation, which may lead to fatigue and ultimate separation. Torsional stress occurs when a portion of the file, usually the tip, binds in the canal and the remainder of the file continues to rotate, thereby creating sufficient torque. The elastic limit is exceeded in the absence of torque control settings and plastic deformation of the endodontic rotary NiTi instrument occurs leading to its eventual fracture/separation (20, 21). Cyclic (flexural) fatigue is attributed to the continuous compressive and tensile forces subjected to the inner and the outer portions of the file during instrumentation, leading to fatigue and file separation (14). According to Haikel et al, as well as Shen et al, cyclic fatigue, not torsional stress, is the major cause of file separations (22, 23). Parashos et al examined 7,159 used and discarded rotary NiTi instruments and found the incidence of file fracture to be 5%. Furthermore, 70% of those were attributed to flexural fatigue and 30% to torsional fatigue (12). Cyclic fatigue is dependent on the radius of curvature the file encounters, as well as the diameter and taper of the instrument (14, 22).

With the idea in mind that cyclic fatigue is the most important factor in instrument separation; manufacturers are designing rotary NiTi files with greater resistance to cyclic fatigue as an improvement in product design. Currently, Brasseler (Savannah, GA) markets a NiTi rotary

file EndoSequence™. The EndoSequence™ is a reamer-like instrument with a precision tip and alternating contact points (ACP), as well as a variable pitch that the manufacturer claims keeps the file centered within the canal and prevents transportation or threading into the canal space. Furthermore, the file design does not incorporate radial land areas, the absence of which aids in reducing the friction or lateral resistance against the internal walls of the root canal during instrumentation and in turn, reduces the torque requirements placed on the rotary NiTi file. This enables the file to be operated at a higher speed, rendering it more efficient (24-26). Moreover, EndoSequence™ rotary NiTi files are chemically treated, a process known as electropolishing, to remove surface imperfections and irregularities such as milling grooves, pits, cracks and pits created during the machining process which can potentially serve as crack initiation sites and stress points on the instrument for crack propagation (27, 28). Anderson et al found that electropolished rotary NiTi endodontic files exhibit fewer surface imperfections and irregularities than those that are not electropolished. They further demonstrated that electropolishing had an enhanced effect on the cyclic fatigue life of endodontic NiTi rotary files (29). However, several other studies have shown that electropolishing does not prevent the development of microfractures and in turn, does not make the file more resistant to cyclic fatigue (21, 30-32).

Recently, a new NiTi rotary file system marketed under the name Profile® Vortex™ has been introduced by Dentsply (Densply Tulsa Dental Specialties, Tulsa, OK). This NiTi file has been manufactured with the M-Wire alloy technology that was initially used in the GT® Series X™ file. M-Wire used to manufacture the Profile® Vortex™ file is a variant NiTi alloy that has undergone a proprietary method of treatment that involves sequential heating and annealing of the conventional 508 Nitinol alloy (33). This process results in a material that is in both a

martensite and premartensite R phase, while at the same time maintaining its pseudoelastic state (21). Due to this process, the manufacturers claim that endodontic rotary NiTi files designed with this technology exhibit an enhanced resistance to file fatigue. Several studies have demonstrated that rotary NiTi files manufactured with M-Wire display a significantly greater resistance to cyclic fatigue than its former Nitinol counterpart (21, 34, 35).

The purpose of this study was to determine the number of rotations to fracture (cyclic fatigue) of the Profile® Vortex™ files compared to the EndoSequence™ files using an *in-vitro* apparatus simulating a curved canal.

Materials and Methods

A total of 200 Profile® Vortex™ files of 25mm length were equally divided into ten groups. Each group represents one of the ten Profile® Vortex™ files (20/0.04, 20/0.06, 25/0.04, 25/0.06, 30/0.04, 30/0.06, 35/0.04, 35/0.06, 40/0.04, and 40/0.06). These ten groups were compared to 200 EndoSequence™ files (Brasseler, Savannah, GA) of 25mm length equally divided into ten groups of tip and taper sizes consistent with the Profile® Vortex™ file groups.

The method used to test time to fracture is similar to that used by Kitchens et al (36). An apparatus was fabricated to simulate a consistent curve inside a canal. A 2.5 in. x 1 in. x 3mm block was made from hardened steel and polished chrome. The block possessed a 2mm wide groove machined into the face to keep the file in position during testing. A 6 in. aluminum baseplate and adjustable block holder was attached to the baseplate of an Instron machine (Instron corp., Canton, MA) and set to replicate an endodontic file at a consistent angle for each of the groups compared. This angle was measured using the Schneider method and was set at 33 degrees to the slope of the ramp. This method defines the curvature as the angle between a line parallel to the long axis of the canal, and another line from the apical foramen to the intersect point with the first line, at the point where the canal begins to leave the long axis of the canal (19) (Figure 1). The groove in the metal block was lubricated with Glyde (Dentsply Maillefer, Ballaigues, Switzerland) prior to each file being tested.

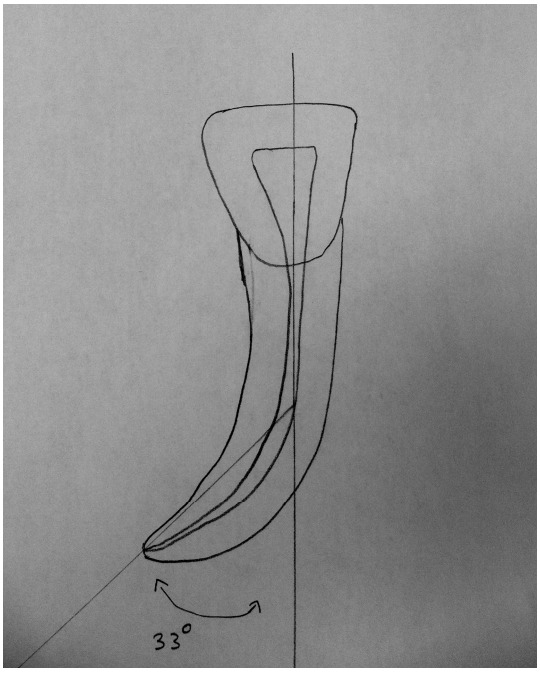

Figure 1: Sketch Depicting Schneider Angle

An electric motor (Aseptico Endo ITR, Aseptico Inc., Woodinville, WA) with an 8:1 contra-angle handpiece (Anthogyr, Aseptico Inc.,Woodinville, WA) was placed in a custom jig fabricated to attach to the Instron testing machine (Figures 2 and 3). Product guidelines from both manufacturers recommended a rotation speed of 500 rpm, therefore, each file was rotated in the handpiece at 500 rpm until the file separated. The time period between the initiation of rotation and fracture was measured with a stopwatch in seconds. The number of instrument rotations completed before separation occurred was calculated [time to fracture x speed] and compared.

The significance of each brand of files with corresponding tip and taper combination was analyzed using a three-way ANOVA followed by specific post-hoc contrasts comparing the two brands for each tip/taper combination. The analyses were performed using SAS software (JMP version 9.0, SAS Institute Inc., Cary NC). The significance level was alpha = 0.05.

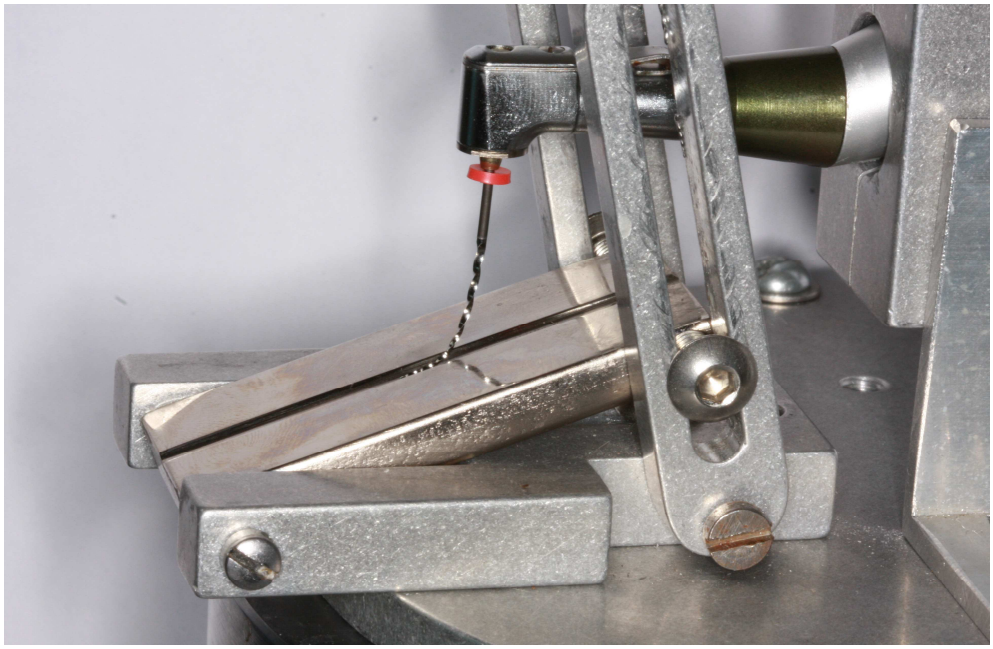

Figure 2: EndoSequence™ Rotary File 30/0.04 in Testing Apparatus

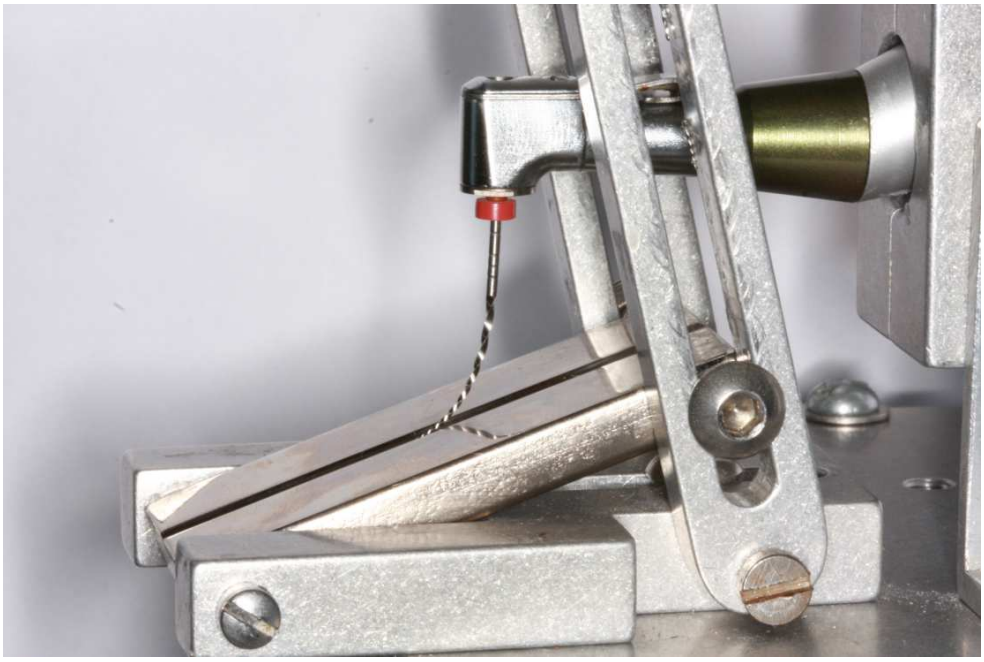

Figure 3: Profile® Vortex™ Rotary File 30/0.04 in Testing Apparatus

Results

The number of rotations until failure was skewed (not in a normal distribution) therefore; the log-transformed values were used for analysis. The log transformed values satisfied the assumptions of ANOVA, equal variability and normality. A three-way ANOVA was used with the following effects in the model: two different brands, five tip sizes and two tapers. An interaction test determined whether the brand differences were consistent across all tip/taper combinations. After the establishment of group differences by ANOVA, at alpha = 0.05, specific post-hoc contrasts compared the two brands for each tip/taper combination.

The number of rotations to failure for each of the twenty groups of files is shown in Table 1. The geometric mean is calculated from the log-transformed time to failure and is shown for each tip, taper and brand combination with 95% confidence interval (CI). For each tip and taper combination, the two brands are compared and the result of this comparison is shown with the p-value in the right column. The significant three-way interaction indicated that the effect of size and taper differed depending upon the manufacturer ($p < .0001$). That is, as may be seen in Figures 4 and 5, the non-parallel lines indicate that the difference between the brands depend upon size and taper chosen.

For the tip/taper combination 20/0.04, the Profile® Vortex™ files' rotations to failure ranged from 1700 to 2758 with a geometric mean rotation to failure of 2289.6 rotations. In the same tip/taper combination, the EndoSequence™ files' rotations to failure ranged from 483 to

1367 with a geometric mean of 671.6 rotations. For the 20/0.04, the Profile® Vortex™ file rotated 3.41 times longer than the corresponding EndoSequence™ file prior to fracture. This value was statistically significant ($p < .001$). For the tip/taper combination 20/0.06, the Profile® Vortex™ files' rotations to failure ranged from 508 to 867 with a geometric mean of 668 rotations. In the same tip/taper combination, the EndoSequence™ files' rotations to failure ranged from 217 to 333 with a geometric mean of 279.9 rotations. For the 20/0.06, the Profile® Vortex™ file rotated 2.39 times longer than the corresponding EndoSequence™ file prior to fracture. This value was statistically significant ($p < .001$). For the tip/taper combination 25/0.04, the Profile® Vortex™ files' rotations to failure ranged from 1425 to 2200 with a geometric mean of 1848.8 rotations. In the same tip/taper combination, the EndoSequence™ files' rotations to failure ranged from 367 to 725 with a geometric mean of 480.9 rotations. For the 25/0.04, the Profile® Vortex™ file rotated 3.84 times longer than the corresponding EndoSequence™ file prior to fracture. This value was statistically significant ($p < .001$). For the tip/taper combination 25/0.06, the Profile® Vortex™ files' rotations to failure ranged from 375 to 792 with a geometric mean of 541.8 rotations. In the same tip/taper combination, the EndoSequence™ files' rotations to failure ranged from 200 to 317 with a geometric mean of 254.4 rotations. For the 25/0.06, the Profile® Vortex™ file rotated 2.13 times longer than the corresponding EndoSequence™ file prior to fracture. This value was statistically significant ($p < .001$). For the tip/taper combination 30/0.04, the Profile® Vortex™ files' rotations to failure ranged from 1208 to 2058 with a geometric mean of 1624.5 rotations. In the same tip/taper combination, the EndoSequence™ files' rotations to failure ranged from 300 to 625 with a geometric mean of 433.1 rotations. For the 30/0.04, the Profile® Vortex™ file rotated 3.75 times longer than the corresponding EndoSequence™ file prior to fracture. This value was statistically significant ($p < .001$). For the tip/taper combination 30/0.06, the Profile® Vortex™

files' rotations to failure ranged from 233 to 500 with a geometric mean of 330.2 rotations. In the same tip/taper combination, the EndoSequence™ files' rotations to failure ranged from 192 to 292 with a geometric mean of 229.9 rotations. For the 30/0.06, the Profile® Vortex™ file rotated 1.44 times longer than the corresponding EndoSequence™ file prior to fracture. This value was statistically significant ($p < .001$). For the tip/taper combination 35/0.04, the Profile® Vortex™ files' rotations to failure ranged from 950 to 1750 with a geometric mean of 1436.6 rotations. In the same tip/taper combination, the EndoSequence™ files' rotations to failure ranged from 275 to 683 with a geometric mean of 427.6 rotations. For the 35/0.04, the Profile® Vortex™ file rotated 3.36 times longer than the corresponding EndoSequence™ file prior to fracture. This value was statistically significant ($p < .001$). For the tip/taper combination 35/0.06, the Profile® Vortex™ files' rotations to failure ranged from 83 to 475 with a geometric mean of 267 rotations. In the same tip/taper combination, the EndoSequence™ files' rotations to failure ranged from 83 to 167 with a geometric mean of 125.6 rotations. For the 35/0.06, the Profile® Vortex™ file rotated 2.13 times longer than the corresponding EndoSequence™ file prior to fracture. This value was statistically significant ($p < .001$). For the tip/taper combination 40/0.04, the Profile® Vortex™ files' rotations to failure ranged from 642 to 1317 with a geometric mean of 1116.2 rotations. In the same tip/taper combination, the EndoSequence™ files' rotations to failure ranged from 308 to 508 with a geometric mean of 377.4 rotations. For the 40/0.04, the Profile® Vortex™ file rotated 2.96 times longer than the corresponding EndoSequence™ file prior to fracture. This value was statistically significant ($p < .001$). For the tip/taper combination 40/0.06, the Profile® Vortex™ files' rotations to failure ranged from 92 to 475 with a geometric mean of 292.4 rotations. In the same tip/taper combination, the EndoSequence™ files' rotations to failure ranged from 50 to 83 with a geometric mean of 66.1 rotations. For the 40/0.06, the Profile® Vortex™ file rotated 4.42

times longer than the corresponding EndoSequence™ file prior to fracture. This value was statistically significant ($p < .001$).

As is clear from Figures 4 and 5, the Profile® Vortex™ files in 0.04 taper required significantly greater rotations to failure than the EndoSequence™ at each of the file tip sizes and in both 0.04 and 0.06 tapers ($p < .001$). The Profile® Vortex™ files in 0.06 taper required significantly greater rotations to failure than the Endosequence™ in 0.06 taper at each of the file tip sizes ($p < .001$). Furthermore, within each brand, the 0.04 taper files outperformed the 0.06 taper files, requiring significantly greater rotations to failure at each of the tip sizes ($p < .001$).

Table 1: Rotations to Failure for Each of the Groups of Files (n=20 each)

			Rotations to Failure			
Size	Taper	Brand	Geometric mean	Range	95% CI	p-value
20	0.04	Sequence	671.6	483 - 1367	(610.6 to 738.8)	
		Vortex	2289.6	1700 - 2758	(2081.4 to 2518.5)	
		Ratio	3.41			<.001
	0.06	Sequence	279.9	217 - 333	(254.5 to 307.9)	
		Vortex	668.0	508 - 867	(607.3 to 734.8)	
		Ratio	2.39			<.001
25	0.04	Sequence	480.9	367 - 725	(437.2 to 529.0)	
		Vortex	1848.8	1425 - 2200	(1680.8 to 2033.7)	
		Ratio	3.84			<.001
	0.06	Sequence	254.4	200 - 317	(231.3 to 279.9)	
		Vortex	541.8	375 - 792	(492.6 to 596.0)	
		Ratio	2.13			<.001
30	0.04	Sequence	433.1	300 - 625	(393.7 to 476.4)	
		Vortex	1624.5	1208 - 2058	(1476.8 to 1786.9)	
		Ratio	3.75			<.001
	0.06	Sequence	229.9	192 - 292	(209.0 to 252.9)	
		Vortex	330.2	233 - 500	(300.2 to 363.2)	
		Ratio	1.44			<.001
35	0.04	Sequence	427.6	275 - 683	(388.8 to 470.4)	
		Vortex	1436.6	950 - 1750	(1306.0 to 1580.3)	
		Ratio	3.36			<.001
	0.06	Sequence	125.6	83 - 167	(114.2 to 138.1)	
		Vortex	267.0	83 - 475	(242.7 to 293.7)	
		Ratio	2.13			<.001
40	0.04	Sequence	377.4	308 - 508	(343.1 to 415.1)	
		Vortex	1116.2	642 - 1317	(1014.7 to 1227.8)	
		Ratio	2.96			<.001
	0.06	Sequence	66.1	50 - 83	(60.1 to 72.7)	
		Vortex	292.4	92 - 475	(265.8 to 321.7)	
		Ratio	4.42			<.001

Note: The log-transformed rotations to failure were analyzed using a three-way ANOVA and the least-square mean transformed for presentation in the table.

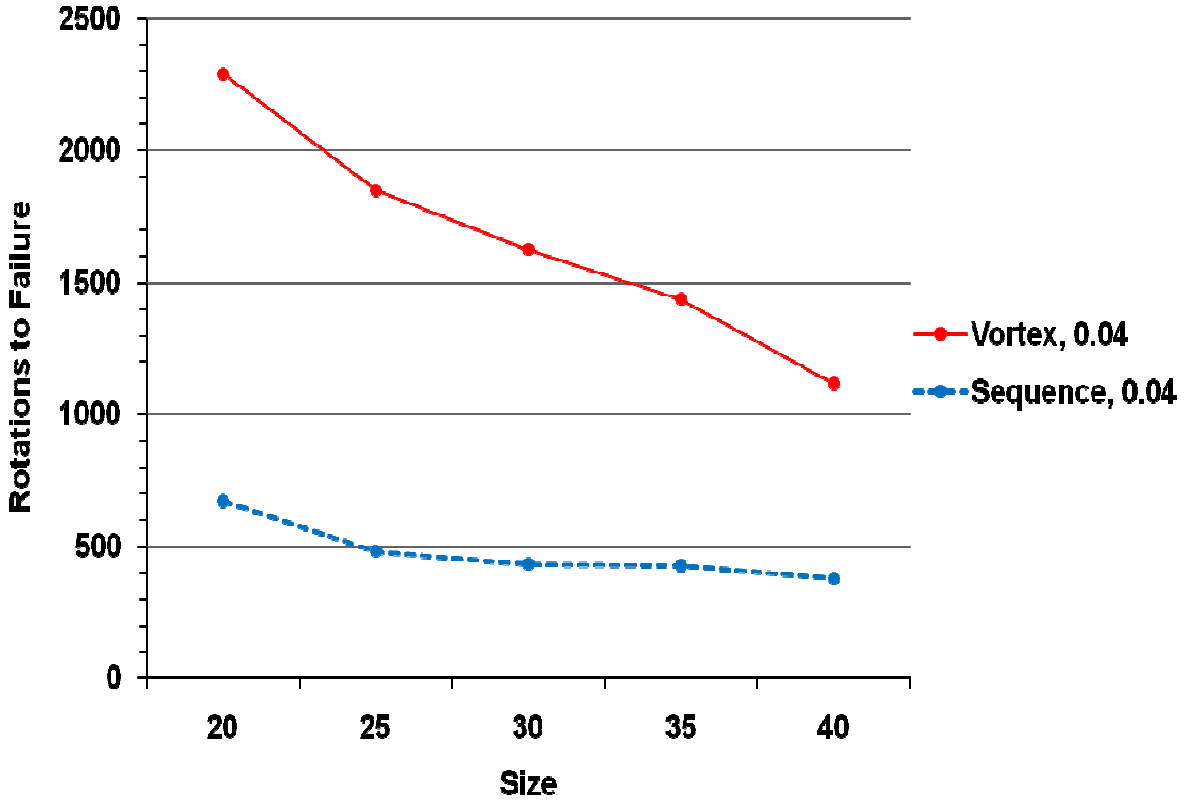

Figure 4: Line Graph Comparison of Profile® Vortex™ to EndoSequence™ in 0.04 Taper

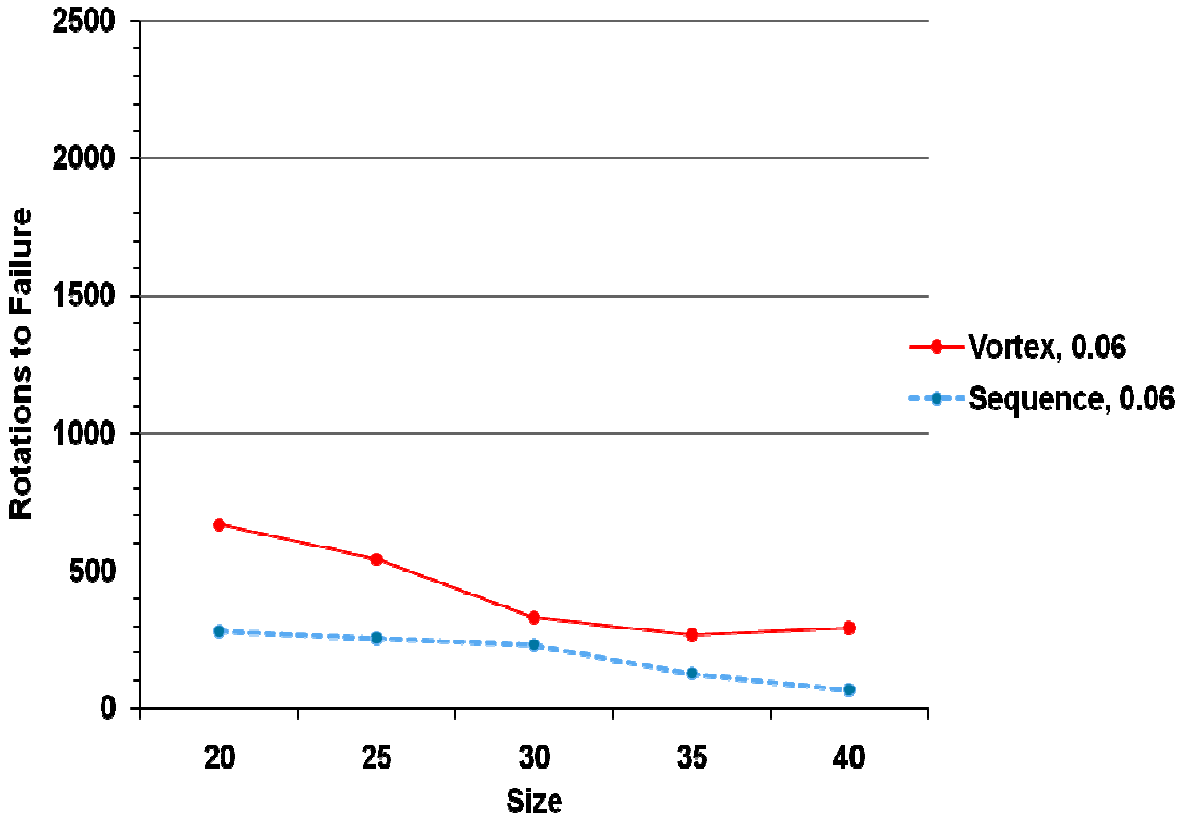

Figure 5: Line Graph Comparison of Profile® Vortex™ to EndoSequence™ in 0.06 Taper

Discussion

The purpose of this study was to determine the number of rotations to fracture (cyclic fatigue) of the Profile® Vortex™ files compared to the EndoSequence™ files (Brasseler USA, Savannah, GA) utilizing an *in-vitro* apparatus simulating a curved canal.

The apparatus designed to simulate a curved canal at a reproducible angle for this study functioned as desired without incident. Files were held in a static position, while allowed to rotate against the metal block of the apparatus, creating tension and compression on the outer and inner aspects of the file respectively at the area of maximum curvature (12, 14). These cumulative compression-tension cycles created with each rotation, resulted in propagation of pre-existing cracks or flaws when the stress reached a critical level and eventually lead to fracture of the instrument (27, 28).

The groove in the metal block (highly polished and lubricated) created a low-friction surface, thus reducing torsional stress as a variable and allowing the authors to focus on cyclic metal fatigue as the only cause of file separation. However, previous studies on simulated root canals using dentin discs have demonstrated that paste and gel-type lubricants such as Glyde are not as effective as an aqueous solution in reducing torque during instrumentation (37) and can actually pose an untoward effect, depending on file design (38). Therefore, the torque generated during rotation of the files might not be as negligible as anticipated. In retrospect, the authors

might have considered utilizing an aqueous solution, sprayed on the metal block while the files were in motion as a lubricant.

The effect of rotational speed on cyclic fatigue of rotary files remains a debatable issue (39). Several *in-vitro* studies have shown that rotational speed has no effect on cycles to fracture (14, 15, 36, 40). In fact, a recent study by Gao and associates compared cyclic fatigue life of Profile® Vortex™ rotary files tested at different rotational speeds (300 rpm and 500 rpm) and found no significant difference between the two speeds, even though the total number of cycles to failure at a speed of 500 rpm was slightly higher than those tested at 300 rpm in both 0.04 and 0.06 tapers (35). Conversely, studies have demonstrated that rotary failure due to cyclic fatigue occurs faster with higher speeds (27) and with fewer cycles (41, 42). Herold et al found that EndoSequence™ NiTi rotary files exhibited a higher rate of separation when rotated at higher speeds (600 rpm compared to 300 rpm) (30). However, based on manufacturer recommendations by both Dentsply and Brasseler, the authors decided to test all the files at a consistent speed of 500 rpm to simulate clinical conditions.

Results in the present study demonstrated that the Profile® Vortex™ files are more resistant to cyclic fatigue fracture than EndoSequence™ in all tip sizes tested and in both tapers. This could be attributed to several factors since there are obvious differences in geometric design, surface condition, raw materials and microstructure between the two brands.

Our results failed to show any positive impact of electropolishing on increased fatigue life as the cycles to fracture of the electropolished EndoSequence™ rotary NiTi files were significantly less than that of the non-electropolished Profile® Vortex™ rotary NiTi files. Our findings in this regard seem to be consistent with previous studies that failed to show superiority of electropolishing relative to NiTi endodontic files that are not electropolished (21, 30-32, 43).

However, since there are several variables in the present study (different geometric file design and raw materials), the authors cannot make a definitive cause and effect relationship between electropolishing and decreased resistance to fracture.

There does seem to be some similarities in the geometric design of the Profile® Vortex™ and the EndoSequence™. Both instruments possess a triangular cross section, absence of radial lands; have varying helical angles and varying pitches to counteract the tendency to thread into the canal wall. However, they exhibit different flexibility and different overall design features.

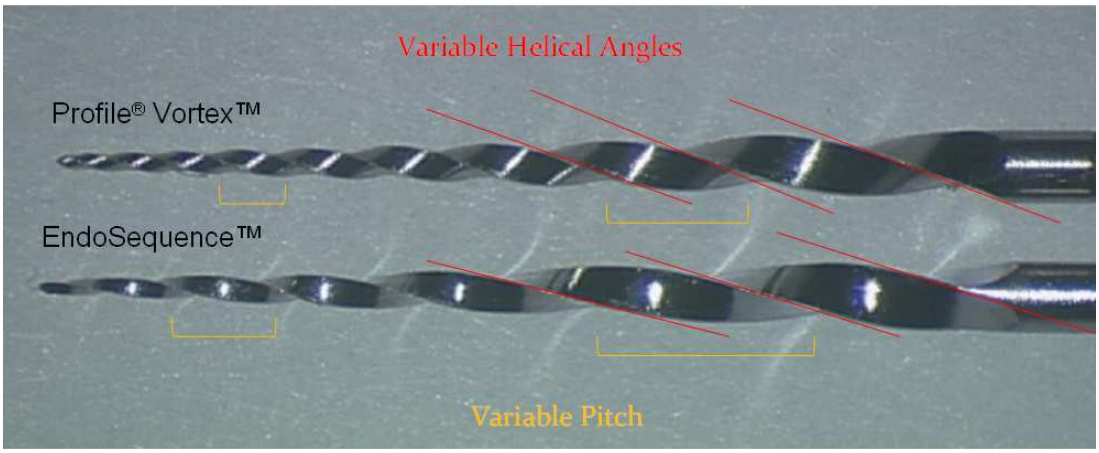

Figure 6: Image Demonstrating Similar Features of Profile® Vortex™ and EndoSequence™ NiTi Rotary Files

The Profile® Vortex™ rotary NiTi file is manufactured from the novel M-wire raw material, which in studies by both Johnson et al and Gao et al, have demonstrated a remarkable resistance to cyclic fatigue and an increased fatigue life of about 400% and 150% respectively, relative to the conventional superelastic Nitinol alloy used in EndoSequence™ (21, 35). The results in the present study found a significant increase in fatigue life of the Profile® Vortex™ rotary NiTi files, relative to the EndoSequence™ and are consistent with previous studies (21, 34,

35, 44). Gambarini and associates did not find any significant difference between M-wire technology and conventional Nitinol alloy in resistance to cyclic fatigue (45).

Previous studies testing for cyclic fatigue resistance seem to be consistent with findings from the present study, when comparing EndoSequence™ to other file systems. In each of these studies, it was concluded that EndoSequence™ rotary NiTi files exhibited significantly lower resistance to cyclic fatigue than the other file systems tested (30, 43). This decrease in resistance could be attributed to certain aspects of the Endosequence™ rotary file design, such as a possible lack of asymmetry in the core diameter of the instrument along its length as well as a possible lack of asymmetry in the position of the alternating contact points (ACP). Subsequent localization of stress at limited points could occur instead of equal distribution of flexibility over the entire cutting length of the NiTi file. Despite the obvious impact of the novel M-Wire alloy and its contributions to increased resistance to fatigue, the authors strongly believe that the design features of the EndoSequence™ played a significant role in the results obtained from the present study.

Results in the present study demonstrated an inversely proportional relationship with regards to taper and cycles to fracture. There was a significant decrease in cycles to fracture and thus less resistance to cyclic fatigue with the 0.06 taper, relative to the 0.04 taper. This was noted in both rotary NiTi rotary file systems (brands) and in all tip sizes. Furthermore, there appeared to be a general trend (although not statistically significant for each file size) within both rotary file systems, revealing a decrease in resistance to cyclic fatigue with progressively larger tip sizes. Both findings were expected and are in agreement with previous studies (14, 22). This consistent finding could be explained by the obvious decrease in flexibility with increased NiTi file diameter rendering them more prone to cyclic fatigue.

Previous *in-vitro* studies by Dederich et al and Li et al have both demonstrated the importance of pecking (axial motion) during instrumentation and the positive impact it creates on cyclic fatigue life through distribution of stress along a greater surface area (27, 46). This finding is further supported by Preutt et al, who suggested that lingering at a single depth in a canal during instrumentation negatively affects the fatigue life of an endodontic instrument (14). In the present study, the authors considered the fact that different rotary file systems might respond differently to stress while flexed in a constant (static) position. The intended method of use in the root canal space places the file in a dynamic state during rotation. Therefore, the method of testing utilized in the present study is not an entirely accurate representation of the motion and the stress rotary NiTi files undergo *in-vivo*.

The axial motion of the file during testing is not the only variation to the true clinical model. To date, there is no single study design testing cyclic fatigue that is a true clinical simulation of intracanal instrumentation. Other factors such as different trajectories of instruments with the same dimensions, excessive space around a file in motion, inaccurate radii and curvatures are all examples of inconsistencies in the variables tested and could explain the wide variation in cyclic fatigue studies. The authors in the present study stress the need for a specification or universal standard to test cyclic fatigue of endodontic rotary instruments as well as introduction of universally accepted testing devices for *in-vitro* testing of cyclic fatigue. This standard would enable manufacturers and researchers to obtain consistency in methodology and achieve more reliable results for safer and efficient clinical use of endodontic rotary files.

Within the limitations of this study, the authors conclude that the Profile® Vortex™ files were more resistant to fracture by cyclic fatigue than the EndoSequence™ in all the tip sizes tested and in both 0.04 and 0.06 tapers.

References

1. Schneider SW. A comparison of canal preparations in straight and curved root canals. Oral surgery, oral medicine, oral pathology. 1971;32(2):271.

2. Ingle JI. Root canal obturation. J Am Dent Assoc. 1956 Jul;53(1):47-55.

3. Peters O. Current challenges and concepts in the preparation of root canal systems: A review. J Endod. 2004;30(8):559.

4. Stewart GG. The importance of chemomechanical preparation of the root canal. Oral Surg Oral Med Oral Pathol. 1955 Sep;8(9):993-7.

5. Siqueira JF,Jr, Lima KC, Magalhaes FA, Lopes HP, de Uzeda M. Mechanical reduction of the bacterial population in the root canal by three instrumentation techniques. J Endod. 1999 May;25(5):332-5.

6. Bystrm A, Sundqvist G. Bacteriologic evaluation of the efficacy of mechanical root canal instrumentation in endodontic therapy. Scand J Dent Res. 1981;89(4):321.

7. Lin LM, Rosenberg PA, Lin J. Do procedural errors cause endodontic treatment failure? J Am Dent Assoc. 2005 Feb;136(2):187,93; quiz 231.

8. Mullaney TP. Instrumentation of finely curved canals. Dent Clin North Am. 1979 Oct;23(4):575-92.

9. Civjan S, Huget EF, DeSimon LB. Potential applications of certain nickel-titanium (nitinol) alloys. J Dent Res. 1975;54(1):89.

10. Walia HM, Brantley WA, Gerstein H. An initial investigation of the bending and torsional properties of nitinol root canal files. J Endod. 1988 Jul;14(7):346-51.

11. Glossen CR, Haller RH, Dove SB, del Rio CE. A comparison of root canal preparations using ni-ti hand, ni-ti engine-driven, and K-flex endodontic instruments. J Endod. 1995;21(3):146.

12. Parashos P, Gordon I, Messer H. Factors influencing defects of rotary nickel-titanium endodontic instruments after clinical use. J Endod. 2004;30(10):722.

13. Iqbal M, Kohli M, Kim J. A retrospective clinical study of incidence of root canal instrument separation in an endodontics graduate program: A PennEndo database study. J Endod. 2006;32(11):1048.

14. Pruett JP, Clement DJ, Carnes DL,Jr. Cyclic fatigue testing of nickel-titanium endodontic instruments. J Endod. 1997 Feb;23(2):77-85.

15. Zelada G, Varela P, Martn B, Bahllo J, Magn F, Ahn S. The effect of rotational speed and the curvature of root canals on the breakage of rotary endodontic instruments. J Endod. 2002;28(7):540.

16. Crump MC, Natkin E. Relationship of broken root canal instruments to endodontic case prognosis: A clinical investigation. J Am Dent Assoc. 1970 Jun;80(6):1341-7.

17. Grossman LI. Fate of endodontically treated teeth with fractured root canal instruments. J Br Endod Soc. 1968 Jul-Sep;2(3):35-7.

18. Spili P, Parashos P, Messer H. The impact of instrument fracture on outcome of endodontic treatment. J Endod. 2005;31(12):845.

19. Panitvisai P, Parunnit P, Sathorn C, Messer H. Impact of a retained instrument on treatment outcome: A systematic review and meta-analysis. J Endod. 2010;36(5):775.

20. Kramkowski T, Bahcall J. An in vitro comparison of torsional stress and cyclic fatigue resistance of ProFile GT and ProFile GT series X rotary nickel-titanium files. J Endod. 2009;35(3):404.

21. Johnson E, Lloyd A, Kuttler S, Namerow K. Comparison between a novel nickel-titanium alloy and 508 nitinol on the cyclic fatigue life of ProFile 25/.04 rotary instruments. J Endod. 2008 Nov;34(11):1406-9.

22. Haikel Y, Serfaty R, Bateman G, Senger B, Allemann C. Dynamic and cyclic fatigue of engine-driven rotary nickel-titanium endodontic instruments. J Endod. 1999 Jun;25(6):434-40.

23. Shen Y, Cheung G, Bian Z, Peng B. Comparison of defects in ProFile and ProTaper systems after clinical use. J Endod. 2006;32(1):61.

24. Koch K, Brave D. Real world endo sequence file. Dent Clin North Am. 2004;48(1):159.

25. Koch K, Brave D. The EndoSequence file: A guide to clinical use. Compend Contin Educ Dent. 2004;25(10A):811.

26. Kurtzman G. Simplifying endodontics with EndoSequence rotary instrumentation. J Calif Dent Assoc. 2007;35(9):625.

27. Li U, Lee B, Shih C, Lan W, Lin C. Cyclic fatigue of endodontic nickel titanium rotary instruments: Static and dynamic tests. J Endod. 2002;28(6):448.

28. Kuhn G, Tavernier B, Jordan L. Influence of structure on nickel-titanium endodontic instruments failure. J Endod. 2001;27(8):516.

29. Anderson ME, Price JW, Parashos P. Fracture resistance of electropolished rotary nickel-titanium endodontic instruments. J Endod. 2007 Oct;33(10):1212-6.

30. Herold KS, Johnson BR, Wenckus CS. A scanning electron microscopy evaluation of microfractures, deformation and separation in EndoSequence and Profile nickel-titanium rotary files using an extracted molar tooth model. J Endod. 2007 Jun;33(6):712-4.

31. Cheung GSP, Shen Y, Darvell B. Does electropolishing improve the low-cycle fatigue behavior of a nickel-titanium rotary instrument in hypochlorite? J Endod. 2007;33(10):1217.

32. Larsen CM, Watanabe I, Glickman G, He J. Cyclic fatigue analysis of a new generation of nickel titanium rotary instruments. J Endod. 2009;35(3):401.

33. Buchanan LS. The new GT series X rotary shaping system: Objectives and technique principles. Dent Today. 2008 Jan;27(1):70, 72, 74 passim.

34. Al-Hadlaq SMS, Aljarbou F, AlThumairy R. Evaluation of cyclic flexural fatigue of M-wire nickel-titanium rotary instruments. J Endod. 2010;36(2):305.

35. Gao Y, Shotton V, Wilkinson K, Phillips G, Ben Johnson W. Effects of raw material and rotational speed on the cyclic fatigue of ProFile vortex rotary instruments. J Endod. 2010;36(7):1205.

36. Kitchens GG,Jr, Liewehr FR, Moon PC. The effect of operational speed on the fracture of nickel-titanium rotary instruments. J Endod. 2007 Jan;33(1):52-4.

37. Boessler C, Peters O, Zehnder M. Impact of lubricant parameters on rotary instrument torque and force. J Endod. 2007;33(3):280.

38. Peters OA, Boessler C, Zehnder M. Effect of liquid and paste-type lubricants on torque values during simulated rotary root canal instrumentation. Int Endod J. 2005;38(4):223.

39. Parashos P, Messer H. Rotary NiTi instrument fracture and its consequences. J Endod. 2006;32(11):1031.

40. Daugherty DW, Gound TG, Comer TL. Comparison of fracture rate, deformation rate, and efficiency between rotary endodontic instruments driven at 150 rpm and 350 rpm. J Endod. 2001;27(2):93.

41. Dietz DB, Di Fiore PM, Bahcall JK, Lautenschlager EP. Effect of rotational speed on the breakage of nickel-titanium rotary files. J Endod. 2000;26(2):68.

42. Lopes H, Ferreira AAP, Elias C, Moreira EJL, de Oliveira JCM, Siqueira J. Influence of rotational speed on the cyclic fatigue of rotary nickel-titanium endodontic instruments. J Endod. 2009;35(7):1013.

43. Ray J, Kirkpatrick T, Rutledge R. Cyclic fatigue of EndoSequence and K3 rotary files in a dynamic model. J Endod. 2007;33(12):1469.

44. Larsen CM, Watanabe I, Glickman GN, He J. Cyclic fatigue analysis of a new generation of nickel titanium rotary instruments. J Endod. 2009 Mar;35(3):401-3.

45. Gambarini G, Grande N, Plotino G, Somma F, Garala M, De Luca M, et al. Fatigue resistance of engine-driven rotary nickel-titanium instruments produced by new manufacturing methods. J Endod. 2008;34(8):1003.

46. Dederich DN, Zakariasen KL. The effects of cyclical axial motion on rotary endodontic instrument fatigue. Oral surgery, oral medicine, oral pathology. 1986;61(2):192.

Appendix

Table 2: Raw Data Collection

Manufacturer	Size	Taper	# Rep.	Seconds
Sequence	20	0.04	1	61
Sequence	20	0.04	2	69
Sequence	20	0.04	3	95
Sequence	20	0.04	4	91
Sequence	20	0.04	5	72
Sequence	20	0.04	6	97
Sequence	20	0.04	7	89
Sequence	20	0.04	8	80
Sequence	20	0.04	9	65
Sequence	20	0.04	10	60
Sequence	20	0.04	11	65
Sequence	20	0.04	12	91
Sequence	20	0.04	13	104
Sequence	20	0.04	14	164
Sequence	20	0.04	15	67
Sequence	20	0.04	16	111
Sequence	20	0.04	17	58
Sequence	20	0.04	18	65
Sequence	20	0.04	19	77
Sequence	20	0.04	20	87
Vortex	20	0.04	1	280
Vortex	20	0.04	2	292
Vortex	20	0.04	3	331
Vortex	20	0.04	4	302
Vortex	20	0.04	5	204
Vortex	20	0.04	6	257
Vortex	20	0.04	7	315
Vortex	20	0.04	8	264
Vortex	20	0.04	9	299
Vortex	20	0.04	10	284

Vortex	20	0.04	11	288
Vortex	20	0.04	12	255
Vortex	20	0.04	13	269
Vortex	20	0.04	14	272
Vortex	20	0.04	15	301
Vortex	20	0.04	16	290
Vortex	20	0.04	17	218
Vortex	20	0.04	18	235
Vortex	20	0.04	19	294
Vortex	20	0.04	20	281
Sequence	25	0.04	1	66
Sequence	25	0.04	2	45
Sequence	25	0.04	3	74
Sequence	25	0.04	4	59
Sequence	25	0.04	5	44
Sequence	25	0.04	6	51
Sequence	25	0.04	7	60
Sequence	25	0.04	8	59
Sequence	25	0.04	9	63
Sequence	25	0.04	10	61
Sequence	25	0.04	11	52
Sequence	25	0.04	12	48
Sequence	25	0.04	13	87
Sequence	25	0.04	14	48
Sequence	25	0.04	15	59
Sequence	25	0.04	16	64
Sequence	25	0.04	17	62
Sequence	25	0.04	18	50
Sequence	25	0.04	19	58
Sequence	25	0.04	20	60
Vortex	25	0.04	1	261
Vortex	25	0.04	2	193
Vortex	25	0.04	3	226
Vortex	25	0.04	4	195
Vortex	25	0.04	5	264
Vortex	25	0.04	6	243
Vortex	25	0.04	7	230
Vortex	25	0.04	8	235
Vortex	25	0.04	9	203
Vortex	25	0.04	10	213
Vortex	25	0.04	11	259
Vortex	25	0.04	12	239
Vortex	25	0.04	13	235

Vortex	25	0.04	14	171
Vortex	25	0.04	15	181
Vortex	25	0.04	16	236
Vortex	25	0.04	17	189
Vortex	25	0.04	18	255
Vortex	25	0.04	19	231
Vortex	25	0.04	20	212
Sequence	30	0.04	1	51
Sequence	30	0.04	2	50
Sequence	30	0.04	3	57
Sequence	30	0.04	4	68
Sequence	30	0.04	5	51
Sequence	30	0.04	6	42
Sequence	30	0.04	7	36
Sequence	30	0.04	8	75
Sequence	30	0.04	9	72
Sequence	30	0.04	10	41
Sequence	30	0.04	11	59
Sequence	30	0.04	12	52
Sequence	30	0.04	13	42
Sequence	30	0.04	14	49
Sequence	30	0.04	15	48
Sequence	30	0.04	16	54
Sequence	30	0.04	17	60
Sequence	30	0.04	18	52
Sequence	30	0.04	19	48
Sequence	30	0.04	20	50
Vortex	30	0.04	1	145
Vortex	30	0.04	2	197
Vortex	30	0.04	3	247
Vortex	30	0.04	4	182
Vortex	30	0.04	5	182
Vortex	30	0.04	6	201
Vortex	30	0.04	7	180
Vortex	30	0.04	8	215
Vortex	30	0.04	9	187
Vortex	30	0.04	10	181
Vortex	30	0.04	11	211
Vortex	30	0.04	12	187
Vortex	30	0.04	13	201
Vortex	30	0.04	14	230
Vortex	30	0.04	15	204
Vortex	30	0.04	16	154

Vortex	30	0.04	17	205
Vortex	30	0.04	18	198
Vortex	30	0.04	19	231
Vortex	30	0.04	20	190
Sequence	35	0.04	1	41
Sequence	35	0.04	2	66
Sequence	35	0.04	3	33
Sequence	35	0.04	4	52
Sequence	35	0.04	5	68
Sequence	35	0.04	6	45
Sequence	35	0.04	7	49
Sequence	35	0.04	8	54
Sequence	35	0.04	9	52
Sequence	35	0.04	10	51
Sequence	35	0.04	11	48
Sequence	35	0.04	12	54
Sequence	35	0.04	13	50
Sequence	35	0.04	14	49
Sequence	35	0.04	15	54
Sequence	35	0.04	16	51
Sequence	35	0.04	17	51
Sequence	35	0.04	18	49
Sequence	35	0.04	19	50
Sequence	35	0.04	20	44
Vortex	35	0.04	1	151
Vortex	35	0.04	2	114
Vortex	35	0.04	3	178
Vortex	35	0.04	4	184
Vortex	35	0.04	5	188
Vortex	35	0.04	6	181
Vortex	35	0.04	7	194
Vortex	35	0.04	8	180
Vortex	35	0.04	9	174
Vortex	35	0.04	10	166
Vortex	35	0.04	11	193
Vortex	35	0.04	12	207
Vortex	35	0.04	13	194
Vortex	35	0.04	14	180
Vortex	35	0.04	15	158
Vortex	35	0.04	16	180
Vortex	35	0.04	17	210
Vortex	35	0.04	18	115
Vortex	35	0.04	19	179

Vortex	35	0.04	20	162
Sequence	40	0.04	1	46
Sequence	40	0.04	2	44
Sequence	40	0.04	3	37
Sequence	40	0.04	4	45
Sequence	40	0.04	5	42
Sequence	40	0.04	6	47
Sequence	40	0.04	7	39
Sequence	40	0.04	8	49
Sequence	40	0.04	9	47
Sequence	40	0.04	10	47
Sequence	40	0.04	11	49
Sequence	40	0.04	12	45
Sequence	40	0.04	13	38
Sequence	40	0.04	14	61
Sequence	40	0.04	15	55
Sequence	40	0.04	16	49
Sequence	40	0.04	17	45
Sequence	40	0.04	18	40
Sequence	40	0.04	19	42
Sequence	40	0.04	20	45
Vortex	40	0.04	1	155
Vortex	40	0.04	2	158
Vortex	40	0.04	3	158
Vortex	40	0.04	4	149
Vortex	40	0.04	5	120
Vortex	40	0.04	6	145
Vortex	40	0.04	7	128
Vortex	40	0.04	8	156
Vortex	40	0.04	9	158
Vortex	40	0.04	10	77
Vortex	40	0.04	11	158
Vortex	40	0.04	12	134
Vortex	40	0.04	13	116
Vortex	40	0.04	14	120
Vortex	40	0.04	15	135
Vortex	40	0.04	16	128
Vortex	40	0.04	17	144
Vortex	40	0.04	18	97
Vortex	40	0.04	19	152
Vortex	40	0.04	20	138
Sequence	20	0.06	1	27
Sequence	20	0.06	2	39

Sequence	20	0.06	3	32
Sequence	20	0.06	4	33
Sequence	20	0.06	5	26
Sequence	20	0.06	6	34
Sequence	20	0.06	7	39
Sequence	20	0.06	8	34
Sequence	20	0.06	9	34
Sequence	20	0.06	10	38
Sequence	20	0.06	11	37
Sequence	20	0.06	12	37
Sequence	20	0.06	13	40
Sequence	20	0.06	14	35
Sequence	20	0.06	15	28
Sequence	20	0.06	16	37
Sequence	20	0.06	17	34
Sequence	20	0.06	18	27
Sequence	20	0.06	19	32
Sequence	20	0.06	20	34
Vortex	20	0.06	1	78
Vortex	20	0.06	2	104
Vortex	20	0.06	3	74
Vortex	20	0.06	4	89
Vortex	20	0.06	5	71
Vortex	20	0.06	6	77
Vortex	20	0.06	7	67
Vortex	20	0.06	8	61
Vortex	20	0.06	9	96
Vortex	20	0.06	10	78
Vortex	20	0.06	11	80
Vortex	20	0.06	12	91
Vortex	20	0.06	13	83
Vortex	20	0.06	14	90
Vortex	20	0.06	15	76
Vortex	20	0.06	16	68
Vortex	20	0.06	17	88
Vortex	20	0.06	18	78
Vortex	20	0.06	19	81
Vortex	20	0.06	20	86
Sequence	25	0.06	1	32
Sequence	25	0.06	2	29
Sequence	25	0.06	3	30
Sequence	25	0.06	4	30
Sequence	25	0.06	5	24

Sequence	25	0.06	6	34
Sequence	25	0.06	7	34
Sequence	25	0.06	8	27
Sequence	25	0.06	9	38
Sequence	25	0.06	10	30
Sequence	25	0.06	11	36
Sequence	25	0.06	12	30
Sequence	25	0.06	13	29
Sequence	25	0.06	14	32
Sequence	25	0.06	15	27
Sequence	25	0.06	16	29
Sequence	25	0.06	17	34
Sequence	25	0.06	18	30
Sequence	25	0.06	19	28
Sequence	25	0.06	20	31
Vortex	25	0.06	1	74
Vortex	25	0.06	2	76
Vortex	25	0.06	3	72
Vortex	25	0.06	4	65
Vortex	25	0.06	5	95
Vortex	25	0.06	6	56
Vortex	25	0.06	7	64
Vortex	25	0.06	8	60
Vortex	25	0.06	9	65
Vortex	25	0.06	10	65
Vortex	25	0.06	11	61
Vortex	25	0.06	12	71
Vortex	25	0.06	13	73
Vortex	25	0.06	14	49
Vortex	25	0.06	15	57
Vortex	25	0.06	16	66
Vortex	25	0.06	17	45
Vortex	25	0.06	18	68
Vortex	25	0.06	19	75
Vortex	25	0.06	20	60
Sequence	30	0.06	1	30
Sequence	30	0.06	2	25
Sequence	30	0.06	3	26
Sequence	30	0.06	4	29
Sequence	30	0.06	5	27
Sequence	30	0.06	6	28
Sequence	30	0.06	7	28
Sequence	30	0.06	8	30

Sequence	30	0.06	9	23
Sequence	30	0.06	10	23
Sequence	30	0.06	11	30
Sequence	30	0.06	12	32
Sequence	30	0.06	13	27
Sequence	30	0.06	14	35
Sequence	30	0.06	15	28
Sequence	30	0.06	16	23
Sequence	30	0.06	17	29
Sequence	30	0.06	18	27
Sequence	30	0.06	19	25
Sequence	30	0.06	20	30
Vortex	30	0.06	1	41
Vortex	30	0.06	2	47
Vortex	30	0.06	3	38
Vortex	30	0.06	4	42
Vortex	30	0.06	5	49
Vortex	30	0.06	6	28
Vortex	30	0.06	7	31
Vortex	30	0.06	8	41
Vortex	30	0.06	9	31
Vortex	30	0.06	10	51
Vortex	30	0.06	11	43
Vortex	30	0.06	12	43
Vortex	30	0.06	13	60
Vortex	30	0.06	14	44
Vortex	30	0.06	15	57
Vortex	30	0.06	16	29
Vortex	30	0.06	17	28
Vortex	30	0.06	18	35
Vortex	30	0.06	19	40
Vortex	30	0.06	20	34
Sequence	35	0.06	1	15
Sequence	35	0.06	2	18
Sequence	35	0.06	3	18
Sequence	35	0.06	4	18
Sequence	35	0.06	5	18
Sequence	35	0.06	6	15
Sequence	35	0.06	7	14
Sequence	35	0.06	8	20
Sequence	35	0.06	9	11
Sequence	35	0.06	10	10
Sequence	35	0.06	11	14

Sequence	35	0.06	12	12
Sequence	35	0.06	13	14
Sequence	35	0.06	14	14
Sequence	35	0.06	15	18
Sequence	35	0.06	16	15
Sequence	35	0.06	17	14
Sequence	35	0.06	18	14
Sequence	35	0.06	19	18
Sequence	35	0.06	20	16
Vortex	35	0.06	1	50
Vortex	35	0.06	2	14
Vortex	35	0.06	3	32
Vortex	35	0.06	4	51
Vortex	35	0.06	5	46
Vortex	35	0.06	6	24
Vortex	35	0.06	7	10
Vortex	35	0.06	8	51
Vortex	35	0.06	9	34
Vortex	35	0.06	10	42
Vortex	35	0.06	11	38
Vortex	35	0.06	12	41
Vortex	35	0.06	13	21
Vortex	35	0.06	14	50
Vortex	35	0.06	15	21
Vortex	35	0.06	16	11
Vortex	35	0.06	17	40
Vortex	35	0.06	18	40
Vortex	35	0.06	19	57
Vortex	35	0.06	20	41
Sequence	40	0.06	1	9
Sequence	40	0.06	2	7
Sequence	40	0.06	3	7
Sequence	40	0.06	4	9
Sequence	40	0.06	5	9
Sequence	40	0.06	6	8
Sequence	40	0.06	7	9
Sequence	40	0.06	8	10
Sequence	40	0.06	9	8
Sequence	40	0.06	10	9
Sequence	40	0.06	11	7
Sequence	40	0.06	12	8
Sequence	40	0.06	13	9
Sequence	40	0.06	14	7

Sequence	40	0.06	15	7
Sequence	40	0.06	16	6
Sequence	40	0.06	17	9
Sequence	40	0.06	18	7
Sequence	40	0.06	19	8
Sequence	40	0.06	20	7
Vortex	40	0.06	1	28
Vortex	40	0.06	2	17
Vortex	40	0.06	3	50
Vortex	40	0.06	4	28
Vortex	40	0.06	5	36
Vortex	40	0.06	6	49
Vortex	40	0.06	7	20
Vortex	40	0.06	8	57
Vortex	40	0.06	9	36
Vortex	40	0.06	10	44
Vortex	40	0.06	11	49
Vortex	40	0.06	12	45
Vortex	40	0.06	13	47
Vortex	40	0.06	14	23
Vortex	40	0.06	15	11
Vortex	40	0.06	16	48
Vortex	40	0.06	17	30
Vortex	40	0.06	18	47
Vortex	40	0.06	19	40
Vortex	40	0.06	20	49

Vita

Dr. Fawaz T. Al-Foraih was born on March 12, 1982 in Kuwait City, Kuwait. He is currently a citizen of Kuwait. Dr. Al-Foraih was enrolled in the Predental program at Virginia Commonwealth University (VCU) where he completed three years prior to dental school. Dr. Al-Foraih received a Doctor of Dental Surgery (DDS) degree in 2006 from VCU. He then went back to Kuwait and completed two years training in an Advanced General Dentistry Internship Program in 2008. Dr. Al-Foraih has since been enrolled in an Advanced Education Program in Endodontics and Masters of Science in Dentistry at VCU. He will graduate from VCU with a Master of Science in Dentistry and a Certificate in Endodontics. Dr. Al-Foraih is a member of the AAE and the Kuwaiti Student Organization. He plans to go back to Kuwait to practice Endodontics for the Ministry of Health.